Volume 54
Number 4
28 January 2025
Pages 1279-1714

Dalton Transactions

An international journal of inorganic chemistry

rsc.li/dalton

ISSN 1477-9226

ROYAL SOCIETY OF CHEMISTRY

FRONTIER

Ming Lu, Yuangang Xu *et al.*

Syntheses and properties of energetic *cyclo*-pentazolate cocrystals

Dalton Transactions

ROYAL SOCIETY OF CHEMISTRY

FRONTIER

View Article Online
View Journal | View Issue

Cite this: *Dalton Trans.*, 2025, **54**, 1307

Syntheses and properties of energetic *cyclo*-pentazolate cocrystals

Fanle Meng,[a] Zihong Ye,[b] Hongwei Zhu,[a] Lianghe Sun,[a] Ming Lu *[a] and Yuangang Xu *[a]

As a new type of polynitrogen species that is stable at room temperature, the pentazolate anion (*cyclo*-N_5^-) has attracted much attention in the field of high-energy density materials, but its energy and stability are unbalanced. Cocrystallisation can balance their properties to some extent by forming new chemical compositions from existing *cyclo*-N_5^- compounds through non-covalent interactions. This article reviews the research progress of *cyclo*-N_5^- cocrystals in recent years, including synthetic methods, cocrystals of metal-N_5^- compounds, and cocrystals of nonmetallic pentazolate salts. The cocrystals of metal-N_5^- compounds mainly include metal-N_5^- solvates, cocrystals composed of metal-N_5^- compounds and amines/MSM, and metal-containing composite salts. The cocrystals of nonmetallic pentazolate salts include cocrystals composed of *cyclo*-N_5^- salts and solvents, cocrystals composed of *cyclo*-N_5^- salts and *N*-heterocyclic molecules, and non-metallic composite salts. The fascinating crystal structures (in some cases topological structures), stable forms, and physicochemical properties of representative cocrystals were highlighted. In addition, the future directions that need to be focused on in this field were pointed out, including the development of more preparation methods, especially those suitable for scaling up; higher precision calculation or testing of enthalpy of formation; improvement of their thermal stabilities; creation of cocrystals of *cyclo*-N_5^- salts and high-density, high-oxygen balance, high-energy oxidizers; and exploration of the formation mechanism.

Received 26th September 2024,
Accepted 15th November 2024

DOI: 10.1039/d4dt02727b

rsc.li/dalton

1 Introduction

High nitrogen energetic materials, as an important class of high-energy density materials (HEDMs), have great potential for military and civilian applications. Among them, polynitrogen species have attracted much attention due to their ultra-high energy and environmental friendliness.[1] The pentazolate

[a]*School of Chemistry and Chemical Engineering, Nanjing University of Science and Technology, Xiaolingwei 200, Nanjing 210094, China. E-mail: luming@njust.edu.cn, yuangangxu@163.com*
[b]*Qian Xuesen College, Nanjing University of Science and Technology, Xiaolingwei 200, Nanjing 210094, China*

Fanle Meng

Fanle Meng received his bachelor's degree from the Jiangsu University of Science and Technology in 2020. He is currently a Ph.D. candidate at the School of Chemistry and Chemical Engineering, Nanjing University of Science and Technology, China. His current research focuses on the design and synthesis of high-nitrogen energetic compounds.

Ming Lu

Ming Lu obtained his BSc in 1984, MSc in 1989 and PhD in 1999 from Nanjing University of Science and Technology. He then became a professor in 2001. He has published more than 200 papers, owns over 10 patents and has authored 5 books. His current research interest is focused on the synthesis and crystal engineering of energetic materials, pharmaceutical intermediates and green chemistry.

anion (*cyclo*-N_5^-) is a pentagon composed entirely of aromatic N–N bonds. Its thermal stability (a thermal decomposition temperature of about 100 °C, with an activation energy of about 100 kJ mol^{-1})[2] is much better than that of the V-shaped N_5^+ cation, and its enthalpy of formation is as high as 3.66 kJ g^{-1} (256 kJ mol^{-1}).[3] The stability and energy of *cyclo*-N_5^- have been accurately predicted by quantum chemistry studies.[4] Over the past half century, extensive theoretical studies and experimental explorations have been carried out on stable HN_5 and *cyclo*-N_5^-; however, the isolation of room-temperature stable *cyclo*-N_5^- compounds has been a great challenge for a long time. It was not until 2017 that Zhang *et al.*[5] successfully synthesized a *cyclo*-N_5^- composite salt $(N_5)_6(H_3O)_3(NH_4)_4Cl$, whose structure was controversial but clearly confirmed the existence of *cyclo*-N_5^- in solid crystals. Subsequently, Xu *et al.*[2] reported a series of metal *cyclo*-N_5^- hydrates. Since then, synthetic studies of *cyclo*-N_5^- derivatives have entered a new phase. At present, the highest detonation velocity of the synthesized *cyclo*-N_5^--containing compounds exceeds 10 000 m s^{-1}, but their density (<1.7 g cm^{-3}) and decomposition temperature (<125 °C) are generally not high, and they also have varying degrees of hygroscopicity.[6] These defects seriously limit the development of *cyclo*-N_5^- based energetic materials, and currently, the commonly used modification methods mainly include coating and doping. However, these methods do not change the internal composition and crystal structure of energetic materials, and the addition of non-energetic components reduces their energetic performance. Therefore, to further improve the modification effect, it is necessary to start from the internal composition and structure of the target molecules and combine the *cyclo*-N_5^- compounds and suitable coformers microscopically in the same crystal lattice through intermolecular non-covalent interactions to form *cyclo*-N_5^--containing cocrystals with enhanced stability and performance.

In recent years, cocrystallization has attracted much attention and has become an effective way to balance the energy and safety of energetic materials.[7] By purposefully introducing a second molecule called a coformer, the intermolecular interactions that determine the stacking arrangement of the target energetic molecule can be disrupted and replaced, resulting in a novel crystal structure called an energetic cocrystal, which incorporates both molecules in a well-defined stoichiometry. Energetic cocrystals have been reported to have improved thermal stability, enhanced detonation properties, and reduced sensitivity to external stimuli.[8] However, while cocrystallization has now been widely studied, the advancement of cocrystallization of energetic ion salts has been slow, with typical examples being 2,4,6,8,10,12-hexanitrate-2,4,6,8,10,12-hexaazaisowoodzane (CL-20) : 1-amino-3-methyl-1,2,3-triazolium nitrate,[9] 2 ammonium dinitramide (ADN) : pyrazine-1,4-dioxide,[10] 2 ammonium nitrate (AN) : 5,5′-dinitro-2*H*,2*H*′-3,3′-bi-1,2,4-triazole (DNBT), and 2 ADN : DNBT cocrystals.[11] The *cyclo*-N_5^- ion carries a negative charge and is not only a good hydrogen bond acceptor but also a planar structure that easily experiences π–π stacking, exhibiting the structural characteristics of cocrystallization. Therefore, *cyclo*-N_5^--containing energetic cocrystals can be formed by suitable coformers to change the molecular composition and crystal structure of *cyclo*-N_5^- salts, increase their decomposition temperatures and densities, reduce their sensitivities, improve their hygroscopicity, and prepare new high-performance and high-stability *cyclo*-N_5^- based energetic materials.

This frontier article reviews the methods for synthesizing *cyclo*-N_5^- containing energetic cocrystals in recent years, their crystal structures, classification, thermal stabilities, energy properties (density, detonation velocity, and detonation pressure), and sensitivities. In order to encourage innovative research on *cyclo*-N_5^- cocrystals, the challenges and application prospects related to them are outlined.

2 Synthetic methods for accessing *cyclo*-N_5^- cocrystals

Cyclo-N_5^- has D_{5h} symmetry, with all of its five nitrogen atoms being sp^2 hybridized.[12] As shown in Fig. 1, it has a dual aromatic skeleton with six π-electrons delocalized in a conjugated manner above and below the *cyclo*-N_5^- ring plane, conferring *cyclo*-N_5^- π-aromaticity; meanwhile, in the equatorial plane of the *cyclo*-N_5^- ring, the lone pair of electrons from the five N atoms leads to flower-like delocalization of the electrons, indicating the σ-aromaticity of *cyclo*-N_5^-. Thus, its unique structure implies good adaptability to form cocrystals with other molecules.

Cocrystal preparation methods include solvent evaporation, solvent/nonsolvent, cooling crystallization, grinding methods,

Yuangang Xu

Yuangang Xu is a professor and doctoral supervisor at the School of Chemistry and Chemical Engineering, Nanjing University of Science and Technology (NJUST). He received his PhD degree in Chemical Engineering and Technology (2020) from NJUST. His research interests include energetic cocrystals, polynitrogen materials, and hydrogen bonding organic frameworks.

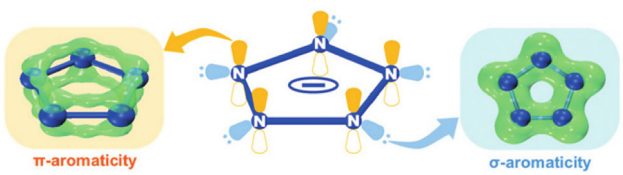

Fig. 1 The dual aromaticity of the *cyclo*-N_5^- ring.

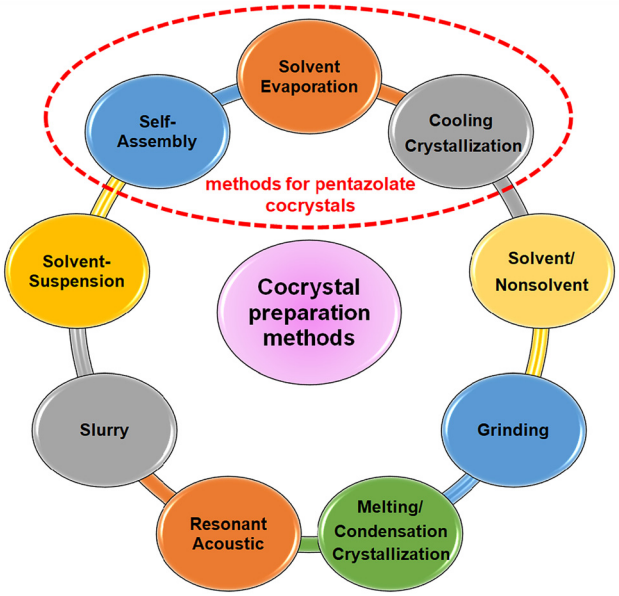

Fig. 2 Synthetic methods of cocrystals.

melting/condensation crystallization, resonant acoustic methods, slurry methods, solvent-suspension methods, and self-assembly methods, all of which have been widely reported thus far (Fig. 2).[13] Currently, there are two main methods for the syntheses of *cyclo*-N_5^- cocrystals: solvent evaporation and self-assembly methods. However, neither method can proceed without a metathesis reaction. Since 2017, our group has reported on metathesis reactions of $[Na(H_2O)(N_5)]\cdot 2H_2O$ with chlorides or nitrates.[2,3] Similar to our work, metathesis reactions of $[Mg(H_2O)_6(N_5)_2]\cdot 4H_2O$ with some sulfates were subsequently developed.[14] However, unless the target product can precipitate, both routes require repeated recrystallization in other cases and are cumbersome and inefficient since NaCl and $MgSO_4$ are difficult to remove completely from commonly used solvents. In 2019, we found that protonation and metathesis reactions can be completed in one pot,[15] but only two *cyclo*-N_5^- hydrates were synthesized. Then metathesis reactions driven by the precipitation of AgCl and $BaSO_4$ were invented in the same year.[16,17] In particular, the method driven by AgCl has the advantages of simple, rapid, high yields, and high universality and has become the most widely used method for synthesizing *cyclo*-N_5^- derivatives. These methods provide a variety of coformers for creating *cyclo*-N_5^- cocrystals.

3 Cocrystals of metal-N_5^- compounds

Cyclo-N_5^- cocrystals can be divided into cocrystals of metal-N_5^- compounds and non-metallic pentazolate salts. Among them, cocrystals of metal-N_5^- compounds can be further divided into three categories: metal-N_5^- solvates, cocrystals composed of metal-N_5^- compounds and amines/MSM, and metal-containing composite salts. Similarly, cocrystals of non-metallic pentazolate salts can also be divided into three categories: cocrystals composed of *cyclo*-N_5^- salts and solvents, cocrystals composed of *cyclo*-N_5^- salts and *N*-heterocyclic molecules, and non-metallic composite salts.

3.1 Metal-N_5^- solvates

Our early research suggested that the coordination of *cyclo*-N_5^- to metals reduces its decomposition barrier in the gas phase, making it kinetically unstable (*e.g.* the thermal and kinetic stabilities have the order of $Fe(N_5)_2$ < $Ni(N_5)_2$ < NaN_5 < *cyclo*-N_5^-).[18,19] Subsequent experiments proved that these metal-N_5^- compounds formed hydrate cocrystals with water molecules through hydrogen bonds and sometimes coordination bonds, improving their stability and safety. To date, 12 metal-N_5^- hydrates (**1–12**) have been synthesized,[2,20–26] of which **4** is also a solvate (Fig. 3). $[Na(H_2O)(N_5)]\cdot 2H_2O$ (**2**) was first reported by Xu *et al.*[2] and is considered the most important precursor for the synthesis of metal hydrates. Two types of hydrogen bonds, O–H···O and O–H···N, constitute the main stabilization mechanism for stabilizing crystal **2** and its *cyclo*-N_5^-, constructing an intralayer 3D hydrogen bond network in **2**.[27] The O–H···O bond is stronger and can stabilize the crystal, while O–H···N is connected with N in *cyclo*-N_5^-, so it mainly stabilizes *cyclo*-N_5^-. For $[M(H_2O)_4(N_5)_2]\cdot 4H_2O$ (M = Mn, Fe, Co, and Zn; **7**, **8**, **10**, **12**), two types of water (*i.e.*, coordinated water (*c*-H_2O) and hydrogen-bonded water (*h*-H_2O)) significantly contribute to stability but *via* different modes (Fig. 4). The role of *c*-H_2O is to bind with M to reduce the interactions between M and *cyclo*-N_5^-, leading to a less active *cyclo*-N_5^- and higher kinetic barriers (E_as) and reaction energies (ΔEs) for its decomposition. The E_as and ΔEs increased by an average of 7.6 and 15.1 kcal mol^{-1}, respectively. Compared with the reactant, *h*-H_2O enforces fewer electrostatic interactions on *cyclo*-N_5^- in the transition state to suppress decomposition, similar to *c*-H_2O.[28]

Some representative cocrystals with different but fascinating structures can be obtained by adjusting the proportion of the coformer (H_2O). The 1D coordination chain in the single-crystal structure of **2** is demonstrated in Fig. 5a, where Xu

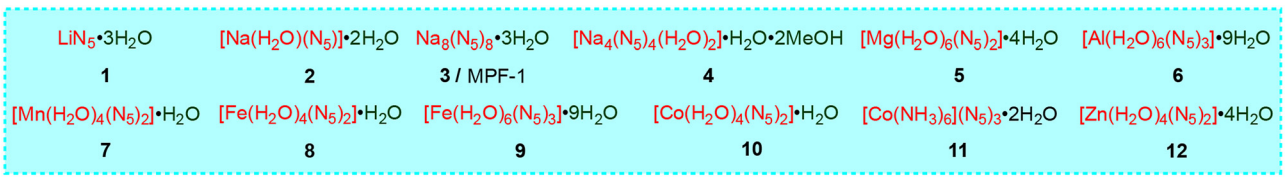

Fig. 3 Metal-N_5^- solvates **1–12**.

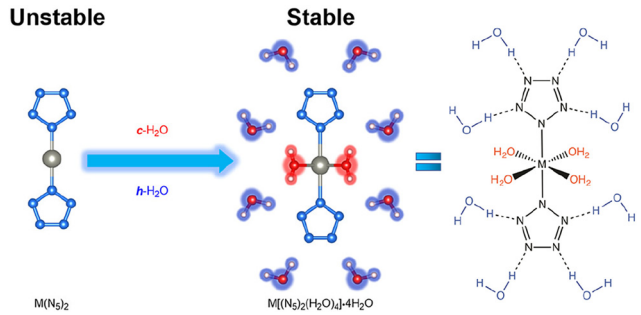

Fig. 4 The two types of first-shell water surrounding and stabilizing an $M(N_5)_2$.

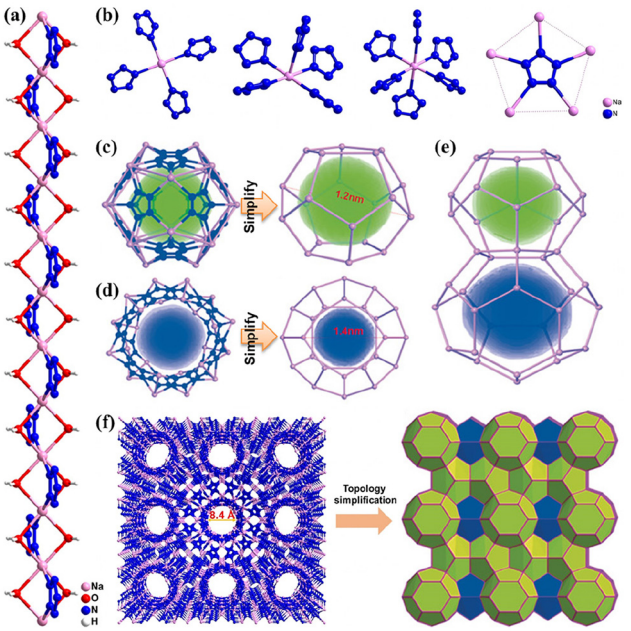

Fig. 5 (a) Single-crystal X-ray structure of **2** (a 1D chain). (b) Coordination environments of Na^+ and *cyclo*-N_5^- in **3**. (c) $Na_{20}N_{60}$ nanocage and simplified 5^{12} topology. (d) $Na_{24}N_{60}$ nanocage and simplified $6^2{\cdot}5^{12}$ topology. (e) Connection mode between the 5^{12} and $6^2{\cdot}5^{12}$ nanocages. (f) 3D framework of **3** and its zeolitic MEP topology.

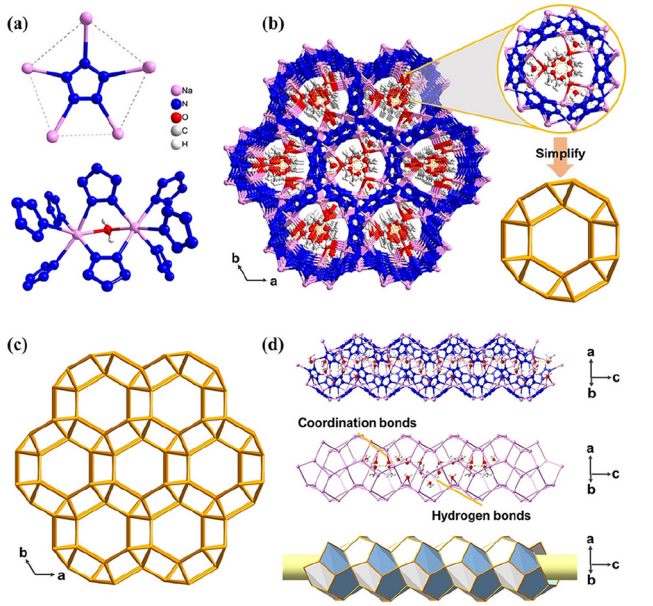

Fig. 6 Single-crystal X-ray structure of **4**. (a) Coordination environments of *cyclo*-N_5^-, Na^+, and water molecules in **4**. (b) 3D framework of **4**, the single channel-like structure, and the simplified topology. (c) The 3D zeolite-like UNJ topological network viewed along the *c* axis. (d) A right-handed double helical chain composed of *cyclo*-N_5^- and Na^+. The hydrogen and coordination bonding interactions in the channels are also shown.

et al.[21] synthesized a new 3D open-framework (**3**/MPF-1) by changing the stoichiometric ratio of NaN_5 to H_2O from 1 : 3 to 8 : 3. Compound **3**/MPF-1 exhibits an aesthetic zeolitic MEP topology featuring two types of nanocages, $Na_{20}N_{60}$ and $Na_{24}N_{60}$, in which the strong coordination bonds between *cyclo*-N_5^- and Na^+ play vital roles in stabilizing the *cyclo*-N_5^- anions (Fig. 5b–f).

The different types of coformers can also lead to different cocrystal structures. Xu *et al.*[23] synthesized a UNJ-type zeolite topology framework, $[Na_4(N_5)_4(H_2O)_2]{\cdot}H_2O{\cdot}2MeOH$ (**4**), by introducing MeOH molecules into **2**. The framework features multiple 1D tubular channels filled with MeOH and H_2O molecules through coordination and hydrogen bonding, whose walls are constructed from Na^+ and *cyclo*-N_5^- (Fig. 6). Each channel is enclosed by six identical channels, indicating that the adjacent nanotubes are fused together by edge sharing. The network has helical channels along the *c*-axis direction. Each enclosed helical channel is assembled from two right-handed helical chains by sharing the sides of multiple pentagons (Fig. 6d).

Due to the low density of the coformer, the crystal densities of cocrystals **1–12** are below 1.7 g cm^{-3}, even at low temperatures.[2,20–26] These cocrystals are stable at room temperature, and most of them have a decomposition temperature of approximately 100 °C (Table 1). Notably, cocrystal **6** has the highest thermal stability among all metal-N_5^- solvates, and studies have shown that hydrogen bonding, van der Waals,

Table 1 Properties of **1–12**

Comp.	d^a (g cm^{-3})	$T_d{}^b$ (°C)
1	1.37 (298 K)	139
2	1.47 (170 K)	104
3	1.30 (100 K)	129
4	1.61 (100 K)	110
5	1.44 (205 K)	104
6	1.38 (150 K)	141
7	1.61 (205 K)	104
8	1.60 (205 K)	115
9	1.43 (193 K)	109
10	1.70 (170 K)	59
11	1.65 (296 K)	102
12	1.67 (205 K)	108

[a] Density from single-crystal X-ray diffraction. [b] Decomposition temperature (DSC).

and π–π stacking interactions play significant roles in the stabilization mechanism.[24] Cocrystals **1** and **3** also exhibit remarkable thermal decomposition temperatures, reaching 139 °C and 129 °C, respectively. In contrast, the decomposition temperature of **10** is only 59 °C, which may be due to the stronger interaction between Co^{2+} and *cyclo*-N_5^- (Co–N: 2.122 Å) compared to other complexes. Once *c*-H_2O is lost, *cyclo*-N_5^- undergoes N–N bond cleavage and decomposition.

3.2 Cocrystals composed of metal-N_5^- compounds and amines/MSM

The structural formula of the cocrystals composed of metal-N_5^- compounds and amines/dimethyl sulfone (MSM) is shown in Fig. 7, where three are NaN_5 cocrystals (**13–15**)[29–31] and the other two are AgN_5 cocrystals (**16** and **17**).[32,33] We recently discovered that **13**[29] also has a UNJ-type zeolite topology framework (Fig. 8) similar to that of **4**. The framework features multiple 1D tubular channels filled with 4-amino-1,2,4-triazole molecules through coordination and hydrogen bonds. Each channel is also surrounded by six identical channels, indicating that adjacent nanotubes are fused together through edge sharing. Similar to **4**, the network also has helical channels along the *c*-axis. But each enclosed helical channel is assembled by two left-handed helical chains sharing multiple pentagonal sides (Fig. 8d).

Cao *et al.* obtained two cocrystals, **14** (MPF-2) and **15** (MPF-4), by adding NaN_5 hydrate and MSM at a specific ratio to a DMSO/amine aqueous solution using MSM as a coformer.[30,31] Each *cyclo*-N_5^- ring in **14** bridges Na^+ through η^3, η^4, and η^5 coordination modes to form a "chiral bowl-shaped" $Na_{16}N_{50}$ molecular container (Fig. 9). These containers are sealed and assembled by parallel arranged trapezoidal 1D helical chains through a 2D chiral layer "molecular plane" formed by sharing *cyclo*-N_5^-. Each container has an ovoid cavity with a volume of approximately 13.4 × 9.1 × 8.8 $Å^3$ occupied by one DMSO guest molecule fixed by hydrogen bonds. It is worth mentioning that the $Na_{16}N_{50}$ bowl in **14** is closely related to the $Na_{20}N_{60}$ (simplified 5^{12}) nanocage in **3**, which is formed by removing 4 Na^+ vertices from the 5^{12} nanocage (Fig. 9c). Both 4-amino-1,2,4-triazole and MSM can be regarded as bidentate ligands, but the stoichiometric ratios of NaN_5 to them in their cocrystals (**13**, **15**) are different (2 : 1 *vs.* 3 : 1). Even more surprising, both of these cocrystals have a

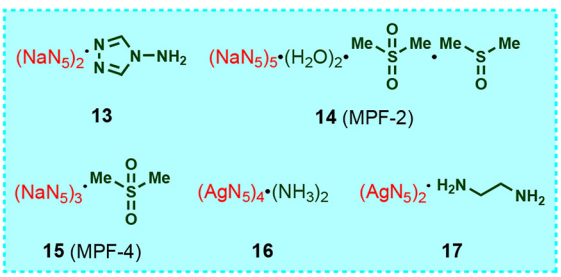

Fig. 7 Cocrystals (**13–17**) composed of metal-N_5^- compounds and amines/MSM.

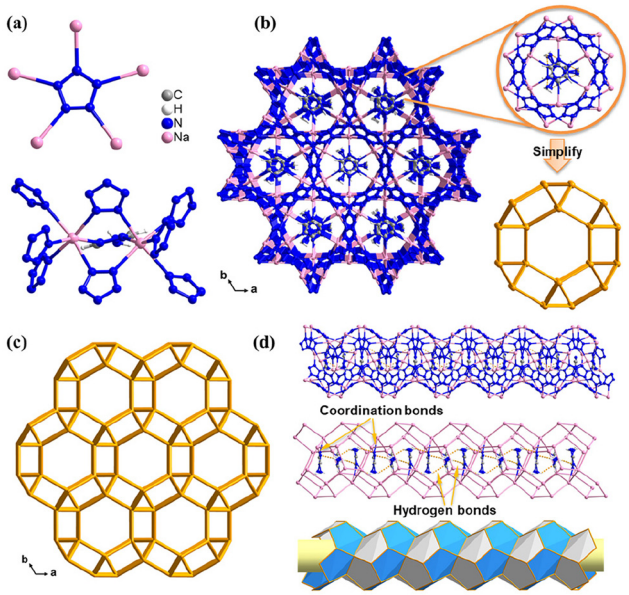

Fig. 8 Single-crystal X-ray structure of **13**. (a) Coordination environments of *cyclo*-N_5^-, Na^+, and 4-amino-1,2,4-triazole molecules in **13**. (b) 3D framework of **13**, the single channel-like structure, and the simplified topology. (c) The 3D zeolite-like UNJ topological network viewed along the *c* axis. (d) A left-handed double helical chain composed of *cyclo*-N_5^- and Na^+. The hydrogen and coordination bonding interactions in the channels are also shown.

homochiral framework with two left-handed helices interpenetrating each other to form a UNJ topology (Fig. 10). Since the structure of **15** is extremely similar to that of **13**, we do not discuss it in detail here.

AgN_5 [34] is one of the most important intermediates for the syntheses of various *cyclo*-N_5^- energetic materials. In order to improve the thermal stability and safety performance of AgN_5, cocrystals **16** and **17** were synthesized (Fig. 11).[32,33] Their coformers are all amines, and their stoichiometric ratio to AgN_5 is 1 : 2. Similar to AgN_5, there are also two types of coordinated Ag^+ (different connected configurations) in **16**. However, only one type of Ag^+ was observed in **17**. Besides, only one type of *cyclo*-N_5^- ring is present in AgN_5 and **17**, while in **16**, there are two types of *cyclo*-N_5^- rings that are coordinated to three and four Ag^+ ions. Moreover, the π–π interactions between *cyclo*-N_5^- anions in AgN_5 are much stronger than those in **16** and **17**. Therefore, the 3D frameworks of **16** and **17** are different from that of AgN_5 (PtS topology). The negatively charged 3D supramolecular framework $Ag_3(N_5)_4$ in **16** is regularly filled with Ag $(NH_3)_2^+$ counter ions by hydrogen bonds, while the 2D AgN_5 networks in **17** are connected layer-by-layer by ethylenediamine molecules through Ag–N coordination bonds, thereby forming a regular 3D supramolecular network.

The crystal densities of two AgN_5 cocrystals (**16** and **17**) are higher than those of three NaN_5 cocrystals (**13–15**), with the highest density of **16** reaching 3.21 g cm^{-3} (Table 2). However, the thermal stabilities of **16** and **17** (≤105 °C) are worse than those of **13–15** (119–127 °C). The detonation velocities (*D*: 6427 and 6272 m s^{-1}) and detonation pressures (*P*: 29.00 and 23.51 GPa) of

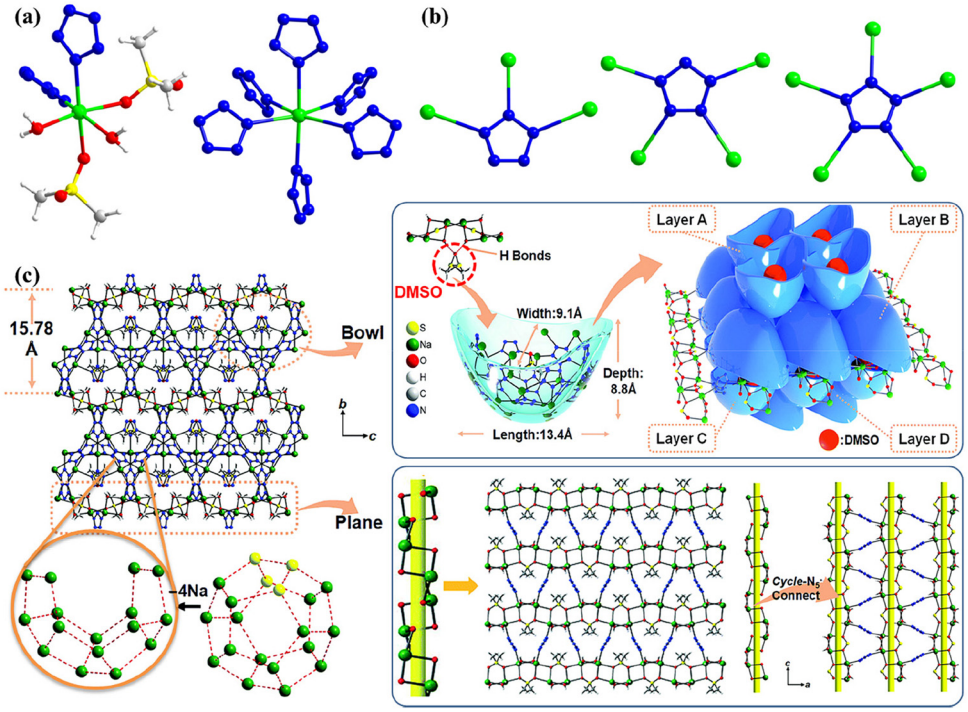

Fig. 9 Single-crystal X-ray structure of **14**. (a) Coordination environments of Na^+ in **14**. (b) Coordination modes of *cyclo*-N_5^- in **14**. (c) The 3D framework of **14** viewed along the *a* axis, and the schematic drawing of the assembly of the bowl and plane.

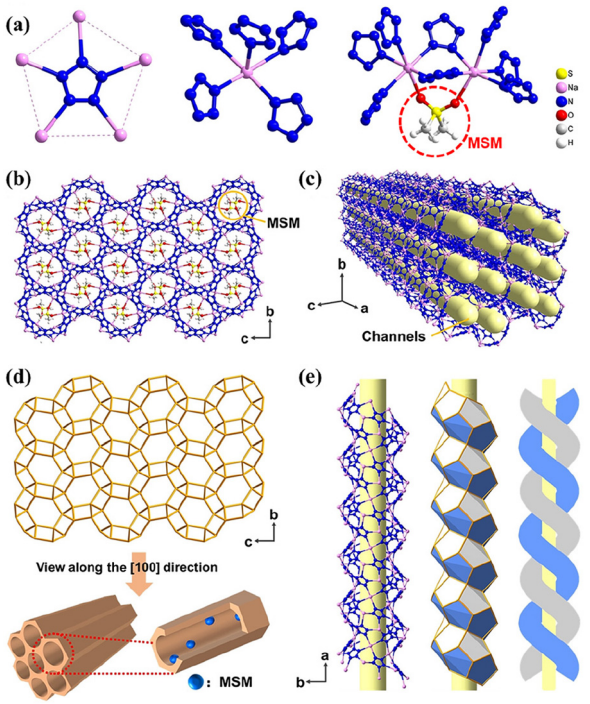

Fig. 10 Single-crystal X-ray structure of **15**. (a) Coordination environments of *cyclo*-N_5^-, Na^+, and MSM molecules in **15**. (b) 3D framework of **15** viewed along the *a* axis. (c) Tubular channels composed of *cyclo*-N_5^- and Na^+ running along the *a* axis. (d) The zeolite-like UNJ topological network and a schematic drawing of the channel structures. (e) A left-handed double helical chain, the topological representation and a schematic drawing of the double helical chain.

16 and **17** are slightly lower than those of AgN_5. Compared with those of extremely sensitive AgN_5, the mechanical sensitivities of the two cocrystals are significantly reduced (Table 2).

3.3 Metal-containing composite salts

There are 14 metal-containing composite salts in *cyclo*-N_5^- cocrystals, including two (**18**[29] and **19**[35]) with two cations, nine (**20–23**,[25,29,36,37] **26**,[34] **27**,[34] and **29–31**[38]) with two anions, two (**24**[25] and **25**[25]) with three anions, and one (**28**[34]) with two cations and two anions (Fig. 12). Cocrystal **18**, the earliest synthesized metal-containing composite salt, has a zeolite-like 3D framework with a SOD topology. **19** has a 3D heterometallic framework with left- and right-handed helical chains. Although **20** is a byproduct obtained during the synthesis of pentazolate *N*-oxide, we discovered the miraculous effect of coformers containing acetate ions on the structural regulation of metal-N_5^- compounds through the structure of **20** and subsequently developed cocrystals **21** and **22** on the basis of KN_5. The 3D topological network of KN_5 is shown in Fig. 13a, which consists of a number of parallelograms neatly arranged in the framework.[16] Unlike KN_5, **21** has a zeolite-like UNJ topological network through hexagons (Fig. 13b), and cocrystal **22** has the same zeolite-like UNJ topological network through inverted triangles consisting of three small triangles and one hexagonal shape (Fig. 13c).

Cocrystals **23–25** have the same hexaaminocobalt(III) cation $[Co(NH_3)_6]^{3+}$, but with different types and numbers of anions, which crystallize in the monoclinic $C1_2/m1$ (**23**) and $C2/m$ (**24** and **25**) space groups, respectively. However, **30** and **31** have the same $[Pb_4(OH)_4]^{4+}$ cubic cation and number of anions,

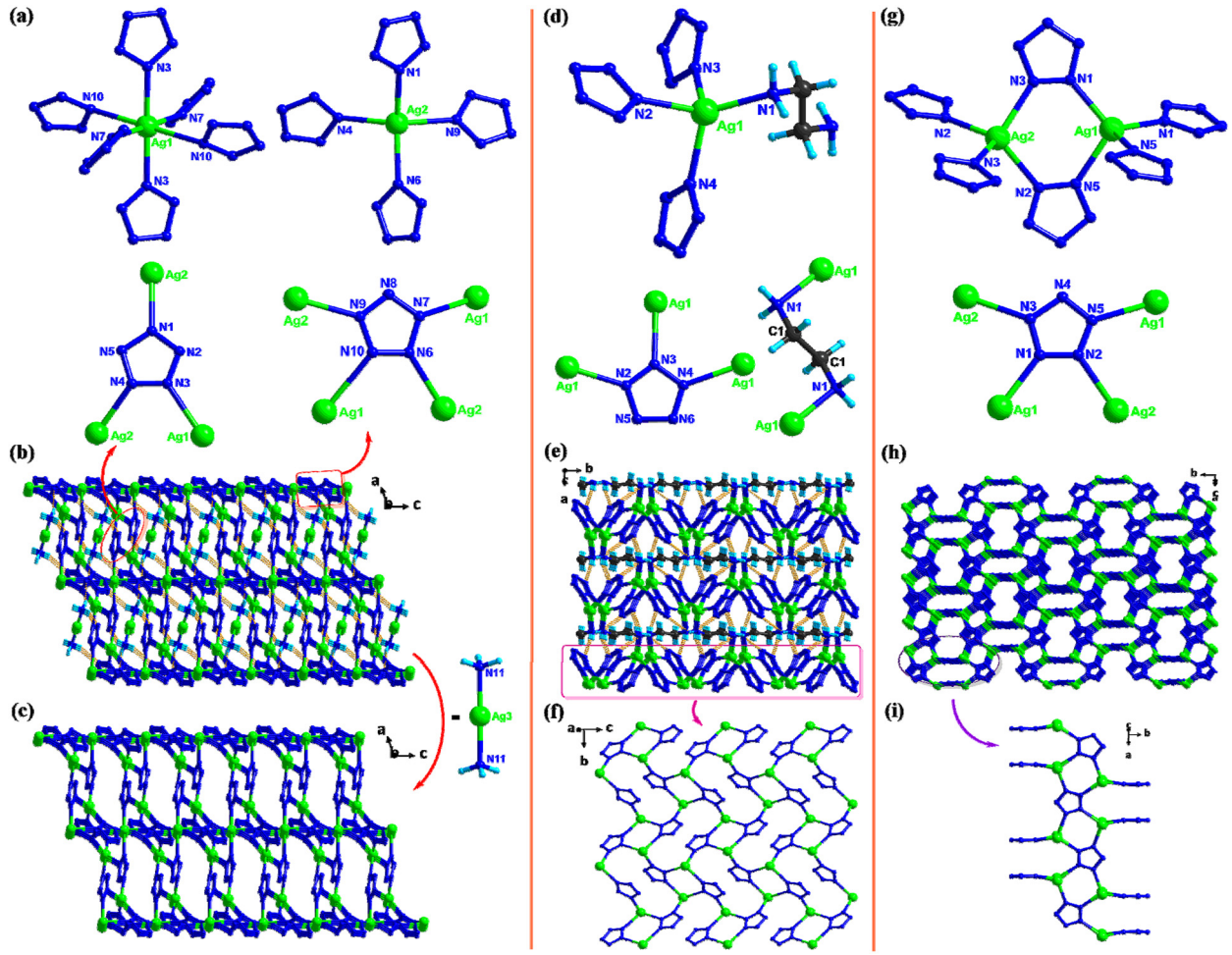

Fig. 11 Single-crystal X-ray structures of **16**, **17**, and AgN_5. (a) Coordination environments of Ag^+ and *cyclo*-N_5^- in **16**. (b) 3D framework of **16**. (c) 3D framework of $Ag_3(N_5)_4$ in **16**. (d) Coordination environments of Ag^+, *cyclo*-N_5^-, and EDA in **17**. (e) 3D framework of **17**. (f) 2D structure in**17**. (g) Coordination environments of Ag^+ and *cyclo*-N_5^- in AgN_5. (h) 3D framework of AgN_5. (i) The 1D structure in AgN_5. Yellow-dashed lines indicate the hydrogen bonds.

Table 2 Properties of **13–17** and AgN_5

Comp.	d^a (g cm^{-3})	$T_d{}^b$ (°C)	D^c (m s^{-1})	P^d (GPa)	IS^e (J)	FS^f (N)
13	1.73 (173 K)	127	7863	26.4		
14	1.65 (296 K)	119				
15	1.66 (295 K)	119				
16	3.21 (220 K)	90	6427	29.00	7.5	60
17	2.73 (170 K)	105	6272	23.51	15	120
AgN_5	3.02 (173 K)	98	7782	34.67	0.5	1

[a] Density from single-crystal X-ray diffraction. [b] Decomposition temperature (DSC). [c] Detonation velocity. [d] Detonation pressure. [e] Impact sensitivity. [f] Friction sensitivity.

except for the types of anions and the number of H_2O. They crystallize in triangular *R*3 (**30**) and orthorhombic $Pca2_1$ (**31**) space groups, respectively. It is worth mentioning that **26** is the only *cyclo*-N_5^- cocrystal composed of only two elements (Cu and N), but once it separates from the mother liquor, it can easily cause an explosion.

The densities of cocrystals **18–31** vary from 1.21 g cm^{-3} to 4.42 g cm^{-3} (Table 3), which is attributed mainly to the types of metal ions, coformed ions, and crystal water content, as well as the resulting differences in the crystal stacking patterns. Among these 14 cocrystals, **25** has the highest thermal decomposition temperature (163 °C), followed by **20** (139 °C) and **27** (130 °C). In order to evaluate the energetic performance of **23**, detonation tests conducted in the literature have shown that the cocrystal has high priming ability and is expected to become a potential green primary explosive.[25]

4 Cocrystals of non-metallic pentazolate salts

4.1 Cocrystals composed of *cyclo*-N_5^- salts and solvents

Hydrates (or solvates) of non-metallic pentazolate salts are very common. On the one hand, cations in non-metallic pentazolate salts are good donors of hydrogen bonds (rich in N–H),

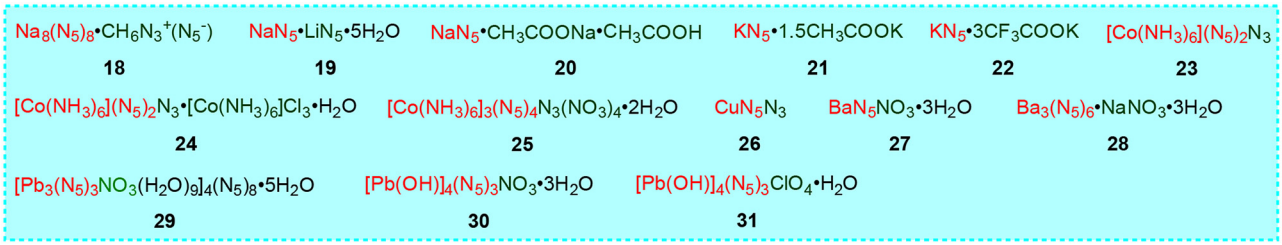

Fig. 12 Metal-containing composite salts **18–31**.

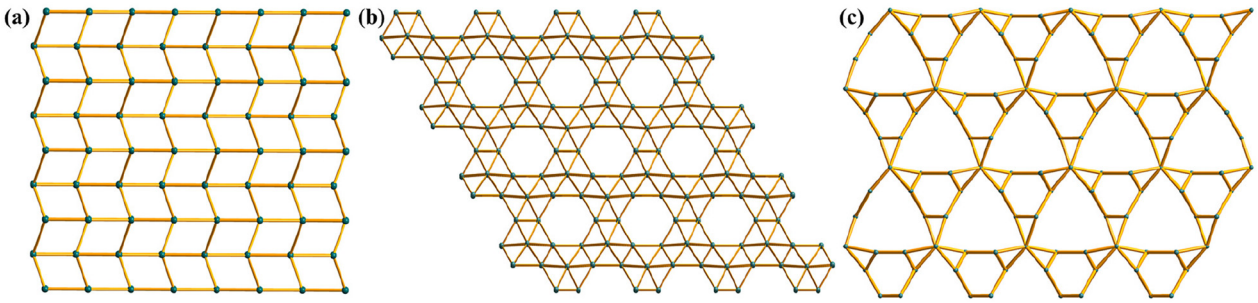

Fig. 13 The 3D topological network of KN_5 (a), **21** (b), and **22** (c).

Table 3 Properties of **18–31**

Comp.	d^a (g cm^{-3})	$T_d{}^b$ (°C)
18	1.21 (170 K)	118
19	1.55 (173 K)	106
20	1.71 (100 K)	139
21	1.75 (298 K)	100
22	2.10 (298 K)	100
23	1.72 (170 K)	98
24	1.63 (296 K)	104
25	1.60 (296 K)	163
26	2.62 (173 K)	90
27	2.59 (100 K)	130
28	2.34 (100 K)	121
29	2.85 (296 K)	89
30	3.91 (296 K)	97
31	4.42 (296 K)	110

[a] Density from single-crystal X-ray diffraction. [b] Decomposition temperature (DSC).

cyclo-N_5^- anions are good acceptors of hydrogen bonds, and water molecules are both excellent donors and acceptors of hydrogen bonds. During the crystallization process, owing to weak interactions or crystal stacking, smaller water molecules are needed to fill the crystal cell to form a cocrystal. On the other hand, water, as a green solvent with a strong ability to dissolve energetic salts, is inevitable in the synthesis of *cyclo*-N_5^- and its conversion to non-metallic salts. Fig. 14 shows the chemical formula of 10 hydrates (or solvates) of non-metallic pentazolate salts (**32–41**)[15–17,39–43] and the stoichiometric ratio of *cyclo*-N_5^- salts to water (or solvent molecules) (1 : 0.5/1/2/3). Among them, **34–36** have $-NH_2$ rich triazolium cations; **37** and **38** have cage-like cations; and **39** and **40** have the same 5/5 fused imidazolium pentazolate. These cocrystals have a density below 1.6 g cm^{-3} and a thermal decomposition temperature of ≤115 °C (Table 4).

One of the strategies for reducing the mechanical sensitivity of highly sensitive energetic materials (such as metal-N_5^- compounds) is to form cocrystals of energetics and solvent molecules.[44] The sensitivities of non-metallic pentazolate salts are moderate, and there is no need to passivate them through hydrates or solvates. Therefore, researchers do not want to obtain hydrates or solvates of non-metallic pentazolate salts, but rather pure salts, to obtain more accurate structures, interactions, and physicochemical properties. However, H_2O_2 is both a solvent and a green oxidizer, with low environmental impact and insensitivity in its solvent form. If H_2O_2 can be embedded into *cyclo*-N_5^- salts with a negative oxygen balance through a solvation strategy, it is expected that the oxygen balance and energy of the developed *cyclo*-N_5^- cocrystal will be correspondingly improved. In 2020, Luo *et al.* successfully produced **41** by utilizing the effective strategy of a CL-20 : H_2O_2 (2 : 1) cocrystal[45] proposed by Matzger *et al.*

In cocrystal **41**, H_2O_2 molecules are incorporated into the crystal lattices of NH_4N_5 to construct a novel 3D hydrogen-bonding network, where *cyclo*-N_5^- rings are layer-by-layer stacked and NH_4^+ cations are embedded in the layers and connected by hydrogen bonding (Fig. 15). This cocrystal has a high oxygen balance and high D and P values (8938 m s^{-1} and 26.37 GPa), which are much higher than those of NH_4N_5. In addition, **41** exhibits an astonishing specific impulse (I_{sp}: 260 s), which is approximately 15% higher than that of NH_4N_5 (225 s). Furthermore, the combustion products of **41** are

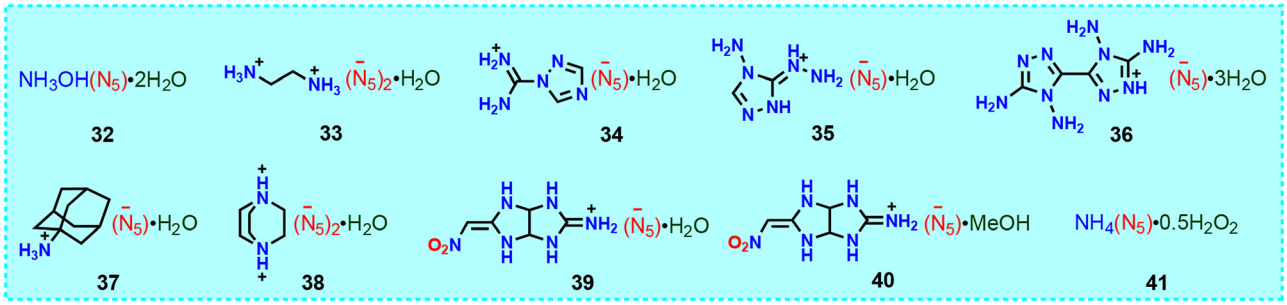

Fig. 14 Cocrystals (**32–41**) composed of *cyclo*-N_5^- salts and solvents.

Table 4 Properties of **32–41**

Comp.	d^a (g cm^{-3})	$T_d{}^b$ (°C)
32	1.49 (173 K)	106
33	1.46 (100 K)	98
34	1.49 (173 K)	96
35	1.58 (170 K)	83
36	1.52 (173 K)	95
37	1.23 (296 K)	79
38	1.48 (293 K)	92
39	1.66 (193 K)	115
40	1.61 (193 K)	115
41	1.49 (295 K)	100

[a] Density from single-crystal X-ray diffraction. [b] Decomposition temperature (DSC). Except for 83 and 100, other data are from the corresponding anhydrous salts.

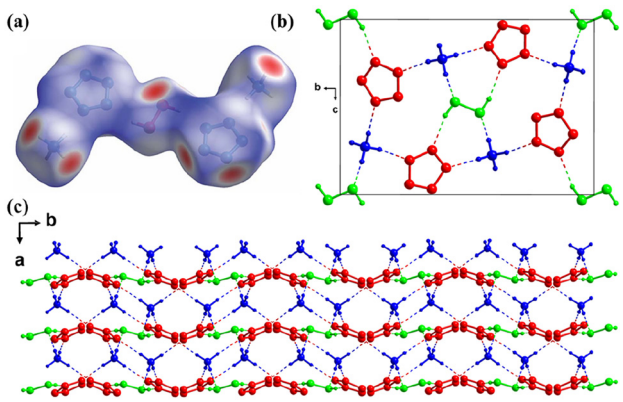

Fig. 15 (a) Single-crystal X-ray structure of **41** (with Hirshfeld surfaces). (b and c) Stacking diagram of **41** viewed along the *a* and *c* axis.

mostly composed of clean N_2, H_2 and H_2O, indicating its great potential as a component of high-energy propellants.

4.2 Cocrystals composed of *cyclo*-N_5^- salts and *N*-heterocyclic molecules

Cocrystals composed of *cyclo*-N_5^- salts and *N*-heterocyclic molecules are relatively rare, with only four cocrystals (**42–45**) being reported (Fig. 16). Therefore, obtaining novel cocrystals of *cyclo*-N_5^- salts with a balance between high energy and

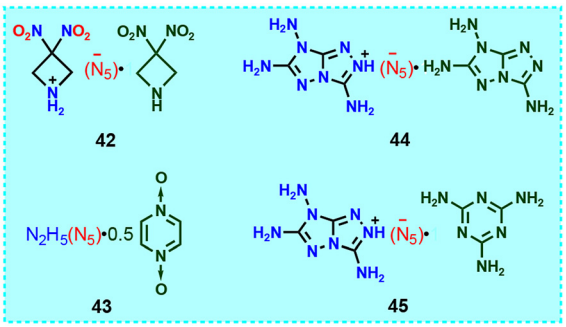

Fig. 16 Cocrystals (**42–45**) composed of *cyclo*-N_5^- salts and *N*-heterocyclic molecules.

good stability is a considerable challenge. The combination of a nonmetallic *cyclo*-N_5^- salt and a neutral molecule in a certain proportion to form a cocrystal compound has a positive effect on the detonation performance and hygroscopic properties of the *cyclo*-N_5^- salt. **42**[46] is a cocrystal composed of 3,3-dinitroazetidine (DNAZ) and $HDNAZ^+N_5^-$ at a 1 : 1 stoichiometry, which is an unexpected product targeting a $DNAZ^+N_5^-$ salt. However, by studying its crystal structure, we found that the crystal is disordered with the H3A proton of the DNAZ cation fixed at 50% occupancy, indicating that the cation is completely occupied and semi-protonated. Therefore, it could be a $(2\ DNAZH)^+N_5^-$ salt.

In order to solve the hygroscopicity problem of $N_2H_5N_5$, pyrazine-1,4-dioxide (PDO) molecules were introduced to synthesize cocrystal **43**, which reduced the moisture absorption of $N_2H_5N_5$ from 45% to 15%.[47] The PDO and *cyclo*-N_5^- rings are parallel, and the distance between them is 3.44 Å, indicating the presence of extensive π–π interactions. There are numerous hydrogen bonds in **43**, which play an important role in the construction of 3D-cube layered stacking (Fig. 17). In addition, after the formation of the cocrystal, the density increased compared with that of $N_2H_5N_5$, but the sensitivity decreased.

Cocrystals **44**[39] and **45**[48] differ only in their coformer, with one being 3,6,7-triamine-7*H*-[1,2,4]triazole[4,3-*b*][1,2,4]triazole (TATOT) and the other being melamine. Both of them have a layered stacking structure, and each *cyclo*-N_5^- in the 2D layer is fixed by seven hydrogen bonds (Fig. 18). Owing to the combined effects of various non-covalent interactions, **45** forms a

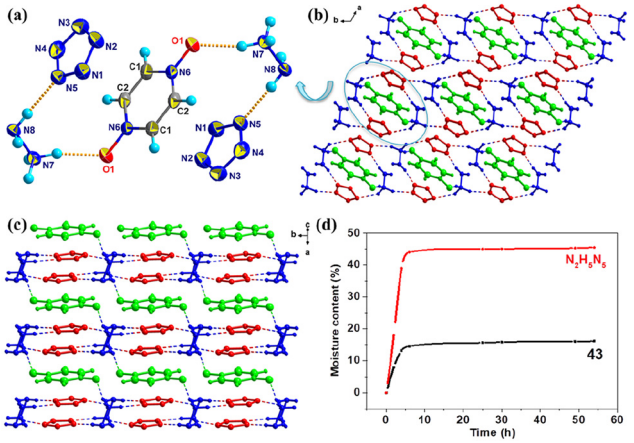

Fig. 17 (a) Single-crystal X-ray structure of **43**. (b and c) Stacking diagram of **43**. (d) Moisture content curves of $N_2H_5N_5$ and **43** under a 75% relative humidity at 25 °C.

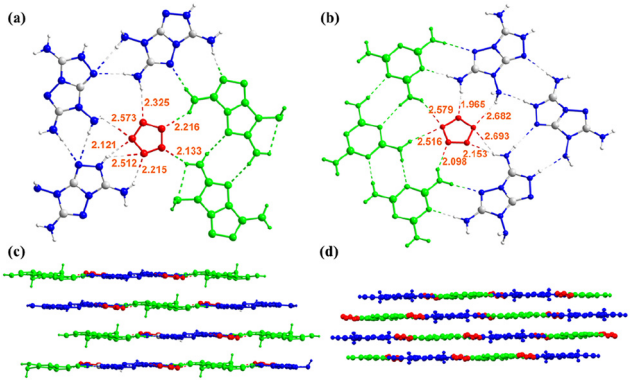

Fig. 18 Single-crystal X-ray structures of **44** and **45**. (a) The position of *cyclo*-N_5^- in the 3 + 2 membered ring and the hydrogen bonds (dotted lines) accepted. (b) The position of *cyclo*-N_5^- in the 3 + 3 membered ring and the hydrogen bonds (dotted lines) accepted. (c) Layer-by-layer stacking of **44**. (d) Layer-by-layer stacking of **45**.

hydrogen-bonded organic framework (HOF) with 1D pores, and *cyclo*-N_5^- rings occupy these pores and are stabilized by hydrogen bonds, π–π interactions between the *cyclo*-N_5^- rings, and attraction between the *cyclo*-N_5^- anions and the cationic HOF. These factors increase its thermal stability to 153 °C (Table 5), exceeding that of **44** (122 °C) and TATOTN$_5$ (121 °C).[16] Overall, the *D* and *P* values of the four cocrystals composed of *cyclo*-N_5^- salts and *N*-heterocyclic molecules are 8029–8735 m s^{-1} and 24.6–29 GPa, respectively (Table 5), which are slightly lower than those of RDX. But they are significantly less sensitive than RDX.

Table 5 Properties of **42–45**

Comp.	d^a (g cm^{-3})	$T_d{}^b$ (°C)	D^c (m s^{-1})	P^d (GPa)	IS^e (J)	FS^f (N)
42	1.67 (193 K)	116	8441	29.0	11	252
43	1.61 (296 K)	101	8735	26.6	35	300
44	1.66 (193 K)	122	8605	26.0	>40	>360
45	1.69 (100 K)	153	8029	24.6	>40	>360

[a] Density from single-crystal X-ray diffraction. [b] Decomposition temperature (DSC). [c] Detonation velocity. [d] Detonation pressure. [e] Impact sensitivity. [f] Friction sensitivity.

4.3 Non-metallic composite salts

The number of non-metallic composite salts of *cyclo*-N_5^- is much less than that of its metal-containing composite salts of only four (**46–49**).[5,15,49,50] Their common feature is that they contain both *cyclo*-N_5^- and Cl^- ions (Fig. 19). Among them, both **46** and **47** crystallize in the cubic $Fd\bar{3}m$ space group, with almost identical unit cell parameters (Fig. 20). Although the unusual structure of **46** was resolved by single-crystal X-ray diffraction analysis, the presence of hydronium ions (H_3O^+) has not been confirmed by other experiments. Thus, a series of debates[51–54] have ensued, such as the correctness of O2 atom assignment, the possible existence of a HN_5 species in this salt, and the pathways and influencing factors for interconversion among HN_5 and *cyclo*-N_5^-.

A comparison of the crystal structures of these two cocrystals revealed the following points. First, the ordered H_3O^+ (O1) in **46** formed only three hydrogen bonds with three *cyclo*-N_5^- rings, but a pair of lone-pair electrons on O1 did not have a hydrogen-bonding interaction with other atoms. The ordered NH_4^+ (N6) in **47**, at the same position as H_3O^+ (O1) in **46**, can form good hydrogen bonds with all the surrounding *cyclo*-N_5^- rings. Second, the isotropic temperature factors of the atomic thermal vibration for the two oxygen atoms, O1 and O2, in **46** are 0.082(3) and 0.071(3), respectively, which are 1.5–2.0 times greater than those of the other atoms (N1–N4 and Cl1). While the thermal vibration temperature factors of all the atoms in **47** are at the same level. Finally, **47** has lower *R* and w*R* indices than **46**, and the goodness-of-fit on F^2 of **47** (1.075) is closer to 1 than that of **46** (1.208). In addition, the correctness of structure **47** was also supported by the experimental results of DSC-TG-MS, SEM-EDX, IR spectroscopy and Raman spectroscopy.

The properties of the four non-metallic composite salts are shown in Table 6. Compared with their corresponding *cyclo*-N_5^- salts, cocrystals **47** and **48** have lower friction and impact sensitivities. Moreover, **47** exhibited better thermal stability (10 °C higher than that of NH_4N_5) and good detonation performance (*D*: 8300 m s^{-1}, *P*: 21.4 GPa) than did FOX-12.[49]

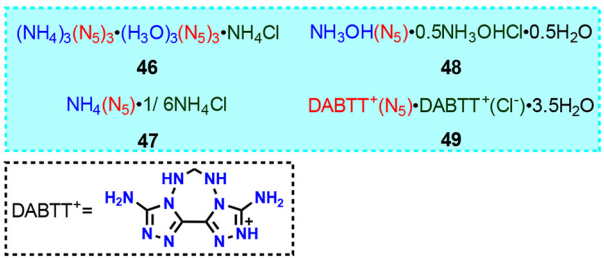

Fig. 19 Non-metallic composite salts **46–49**.

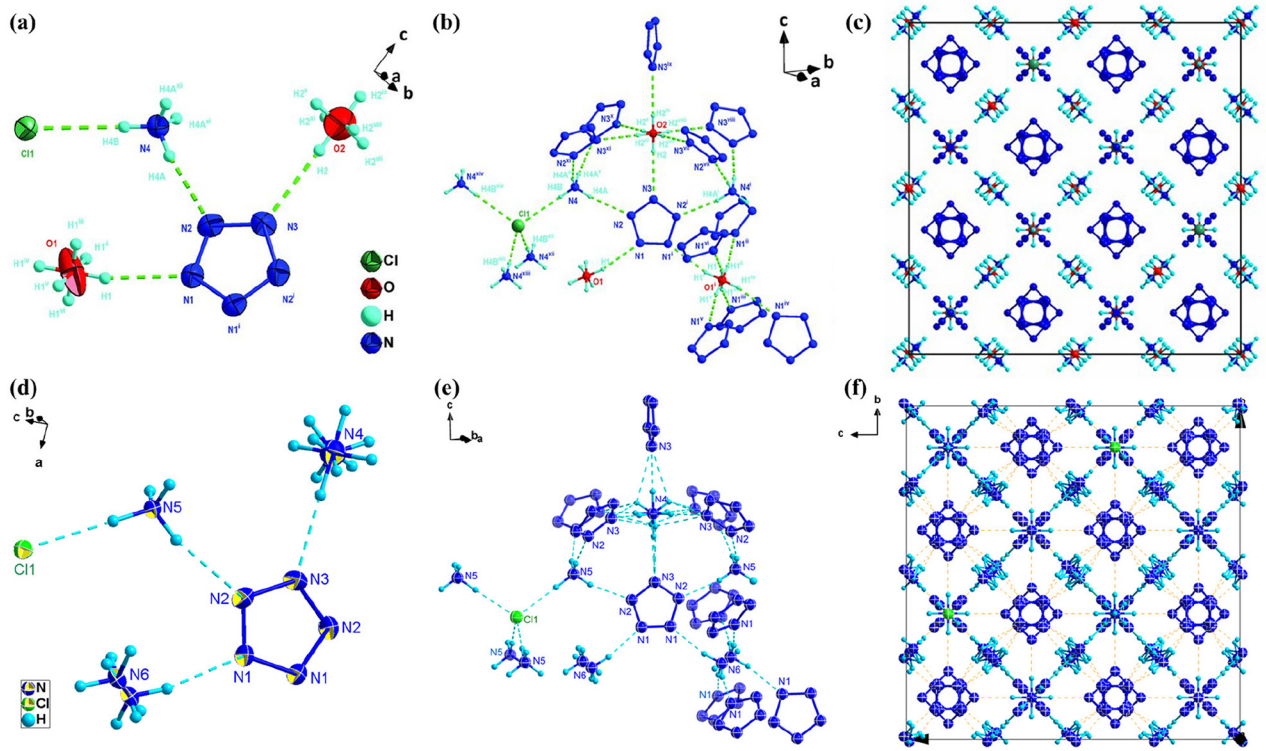

Fig. 20 Single-crystal X-ray structures of **46** and **47**. (a) Single-crystal X-ray structure of **46**. (b) Hydrogen bonds (dotted lines) in the crystal of **46**. (c) Unit cell stacking diagram of **46**. (d) Single-crystal X-ray structure of **47**. (e) Hydrogen bonds (dotted lines) in the crystal of **47**. (f) Unit cell stacking diagram of **47**.

Table 6 Properties of **46–49**

Comp.	d^a (g cm^{-3})	$T_d{}^b$ (°C)	D^c (m s^{-1})	P^d (GPa)	IS^e (J)	FS^f (N)
46	1.34 (123 K)	117				
47	1.34 (150 K)	109	8300	21.4	31	300
48	1.59 (100 K)	95	8260	23.8	>40	>360
49	1.62 (173 K)	99	7615	23.6		

[a] Density from single-crystal X-ray diffraction. [b] Decomposition temperature (DSC). [c] Detonation velocity. [d] Detonation pressure. [e] Impact sensitivity. [f] Friction sensitivity.

5 Summary and outlook

The pentazolate anion and its derivatives represent one of the most important research advances in the field of energetic materials. In the past seven years, many energetic *cyclo*-N_5^- cocrystals have been developed through metathesis reactions combined with solvent evaporation or self-assembly methods. *Cyclo*-N_5^- cocrystals can be divided into cocrystals of metal-N_5^- compounds and non-metallic pentazolate salts according to their composition. Each major category can be further divided into three subcategories: solvates (mainly hydrates), cocrystals composed of *cyclo*-N_5^- compounds and neutral molecules, and composite salts. Among them, metal composite salts represent the largest number (14), followed by solvates of metal (12) and non-metallic salts (10). Overall, the number of water-containing cocrystals (32) accounts for nearly two-thirds of that of *cyclo*-N_5^- cocrystals, and synthesizing anhydrous *cyclo*-N_5^- cocrystals remains a challenge.

Cyclo-N_5^- cocrystals, especially those containing metals, have fascinating crystal structures, including pentasil-zeolite topological networks, metal pentazolate frameworks, and hydrogen-bonded organic frameworks. The thermal stabilities of some cocrystals exceed those of their pentazolate precursors, providing ideas for the development of more promising *cyclo*-N_5^- derivatives.

Suggestions for future key research directions for *cyclo*-N_5^- cocrystals are as follows:

(1) On the basis of the existing synthetic methods for *cyclo*-N_5^- cocrystals, more preparation methods should be developed, especially methods suitable for scale up.

(2) All reported enthalpies of formation of *cyclo*-N_5^- cocrystals were theoretically determined. In order to accurately evaluate their energy, more attention must be paid to using high-precision calculation methods and experimental measurements.

(3) The activation energy barrier for the decomposition of *cyclo*-N_5^- is only about 100 kJ mol^{-1}, so the decomposition temperatures of *cyclo*-N_5^- cocrystals are relatively lower than those of traditional energetic materials such as RDX and HMX. In the direction of application, it is necessary to further increase the thermal stability of *cyclo*-N_5^- cocrystals.

(4) The energetic properties of *cyclo*-N_5^- cocrystals are often between those of the precursors, which means that the energy of a *cyclo*-N_5^- cocrystal is slightly lower than that of a *cyclo*-N_5^- precursor. Therefore, further research is expected to increase the energy through the cocrystallization of *cyclo*-N_5^- compounds and high-density, high-oxygen balance, high-energy oxidizer molecules.

(5) By using advanced methods such as artificial intelligence, machine learning, and high-throughput experiments to study the formation mechanism of *cyclo*-N_5^- cocrystals, we can grasp the key influencing factors of cocrystal formation, which has guiding significance for the future creation of energetic cocrystals and even polynitrogen compounds.

Data availability

No primary research results, software or code have been included and no new data were generated or analysed as part of this review.

Conflicts of interest

There are no conflicts to declare.

Acknowledgements

This work was supported by the National Natural Science Foundation of China (no. 22105102 and 22135003), the Young Elite Scientist Sponsorship Program by CAST (no. YESS20210074), and the Fundamental Research Funds for the Central Universities (no. 30921011204).

References

1 V. E. Zarko, *Combust., Explos. Shock Waves*, 2010, **46**, 121–131.
2 Y. Xu, Q. Wang, C. Shen, Q. Lin, P. Wang and M. Lu, *Nature*, 2017, **549**, 78–81.
3 Y. Xu, Q. Lin, P. Wang and M. Lu, *Chem. – Asian J.*, 2018, **13**, 924–928.
4 D. A. Dixon, D. Feller, K. O. Christe, W. W. Wilson, A. Vij, V. Vij, H. D. B. Jenkins, R. M. Olson and M. S. Gordon, *J. Am. Chem. Soc.*, 2004, **126**, 834–843.
5 C. Zhang, C. Sun, B. Hu, C. Yu and M. Lu, *Science*, 2017, **355**, 374–376.
6 K. Zhong and C. Zhang, *Chem. Eng. J.*, 2024, **483**, 149202.
7 (*a*) J. C. Bennion and A. J. Matzger, *Acc. Chem. Res.*, 2021, **54**, 1699–1710; (*b*) L. M. Foroughi, R. A. Wiscons, D. R. D. Bois and A. J. Matzger, *Chem. Commun.*, 2020, **56**, 2111–2114.
8 (*a*) O. Bolton and A. J. Matzger, *Angew. Chem., Int. Ed.*, 2011, **50**, 8960–8963; (*b*) S. Hanafi, D. Trache, A. Mezroua, H. Boukeciat, R. Meziani, A. F. Tarchoun and A. Abdelaziz, *RSC Adv.*, 2021, **11**, 35287–35299; (*c*) A. Abdelaziz, D. Trache, A. F. Tarchoun, H. Boukeciat, D. E. Kadri, H. Hassam, S. Ouahioune, N. Sahnoun, S. Thakur and T. M. Klapötke, *Chem. Eng. J.*, 2024, **487**, 150654; (*d*) H. Boukeciat, A. F. Tarchoun, D. Trache, A. Abdelaziz, R. Meziani and T. M. Klapötke, *Polymers*, 2023, **15**, 1799.
9 X. Zhang, S. Chen, Y. Wu, S. Jin, X. Wang, Y. Wang, F. Shang, K. Chen, J. Du and Q. Shu, *Chem. Commun.*, 2018, **54**, 13268–13270.
10 M. K. Bellas and A. J. Matzger, *Angew. Chem., Int. Ed.*, 2019, **58**, 17185–17188.
11 A. J. Bennett, L. M. Foroughi and A. J. Matzger, *J. Am. Chem. Soc.*, 2024, **146**, 1771–1775.
12 L. Zhang, C. Yao, Y. Yu, S. Jiang, C. Sun and J. Chen, *J. Phys. Chem. Lett.*, 2019, **10**, 2378–2385.
13 M. Sultan, J. Wu, I. U. Haq, M. Imran, L. Yang, J. Wu, J. Lu and L. Chen, *Molecules*, 2022, **27**, 4775.
14 C. Yang, C. Zhang, Z. Zheng, C. Jiang, J. Luo, Y. Du, B. Hu, C. Sun and K. O. Christe, *J. Am. Chem. Soc.*, 2018, **140**, 16488–16494.
15 Y. Xu, L. Tian, P. Wang, Q. Lin and M. Lu, *Cryst. Growth Des.*, 2019, **19**, 1853–1859.
16 Y. Xu, L. Tian, D. Li, P. Wang and M. Lu, *J. Mater. Chem. A*, 2019, **7**, 12468–12479.
17 L. Tian, Y. Xu, Q. Lin, P. Wang and M. Lu, *Chem. – Asian J.*, 2019, **14**, 2877–2882.
18 X. Zhang, J. Yang, M. Lu and X. Gong, *Struct. Chem.*, 2015, **26**, 785–792.
19 X. Zhang, J. Yang, M. Lu and X. Gong, *RSC Adv.*, 2015, **5**, 21823–21830.
20 Y. Xu, L. Ding, F. Yang, D. Li, P. Wang, Q. Lin and M. Lu, *Chem. Eng. J.*, 2022, **429**, 132399.
21 Y. Xu, P. Wang, Q. Lin, X. Mei and M. Lu, *Dalton Trans.*, 2018, **47**, 1398–1401.
22 W. Zhang, K. Wang, J. Li, Z. Lin, S. Song, S. Huang, Y. Liu, F. Nie and Q. Zhang, *Angew. Chem., Int. Ed.*, 2018, **57**, 2592–2595.
23 Y. Xu, Z. Xu, X. Zhang, T. Hou and M. Lu, *CrystEngComm*, 2022, **24**, 4853–4856.
24 L. Chen, C. Yang, H. Hu, L. Shi, C. Zhang, C. Sun, C. Gao, Y. Du and B. Hu, *CrystEngComm*, 2022, **24**, 8152–8159.
25 Y. Xu, J. Zhou, D. Li, P. Wang, Q. Lin and M. Lu, *Cryst. Growth Des.*, 2022, **23**, 811–819.
26 Y. Xu, P. Wang, Q. Lin and M. Lu, *Dalton Trans.*, 2017, **46**, 14088–14093.
27 X. Li, Y. Long, C. Zhang, C. Sun, B. Hu, P. Lu and J. Chen, *ACS Omega*, 2022, **7**, 6627–6639.
28 J. Luo, L. Chen, D. N. Nguyen, D. Guo, Q. An and M. Cheng, *J. Phys. Chem. C*, 2018, **122**, 21192–21201.
29 P. Wang, Y. Xu, Q. Wang, Y. Shao, Q. Lin and M. Lu, *Sci. China Mater.*, 2018, **62**, 122–129.
30 Y. Cao, S. Huang, Q. Zhang and W. Zhang, *Dalton Trans.*, 2020, **49**, 17542–17546.
31 Y. Cao, H. Xia, K. Wang, Q. Zhang and W. Zhang, *Inorg. Chem.*, 2021, **60**, 8409–8413.

32 X. Zhang, T. Hou, Q. Lin, P. Wang, D. Li, Y. Xu and M. Lu, *CrystEngComm*, 2022, **24**, 1900–1906.
33 C. Sun, C. Zhang, C. Jiang, C. Yang, Y. Du, Y. Zhao, B. Hu, Z. Zheng and K. O. Christe, *Nat. Commun.*, 2018, **9**, 1269.
34 Y. Xu, Q. Lin, P. Wang and M. Lu, *Chem. – Asian J.*, 2018, **13**, 1669–1673.
35 J. Li, K. Wang, S. Song, X. Qi, W. Zhang, M. Deng and Q. Zhang, *Sci. China Mater.*, 2018, **62**, 283–288.
36 Z. Xu, S. Jiang, T. Hou, X. Zhang, M. Lu and Y. Xu, *New J. Chem.*, 2023, **47**, 5616–5620.
37 S. Jiang, J. Zhou, Y. Xu, Q. Lin, P. Wang and M. Lu, *CrystEngComm*, 2024, **26**, 951–956.
38 Y. Yuan, Y. Xu, Q. Xie, D. Li, Q. Lin, P. Wang and M. Lu, *Dalton Trans.*, 2022, **51**, 5801–5809.
39 C. Yang, L. Chen, W. Wu, C. Zhang, C. Sun, Y. Du and B. Hu, *ACS Appl. Energy Mater.*, 2020, **4**, 146–153.
40 S. Chen, C. Yang, C. Sun, C. Zhang, C. Gao, Y. Du and B. Hu, *J. Mol. Struct.*, 2022, **1249**, 131521.
41 T. Jiang, H. Xia, W. Zhang, Z. Cai, S. Song and T. Liu, *CrystEngComm*, 2024, **26**, 977–984.
42 L. Shi, P. Wang, C. Gao, C. Zhang, Y. Du, C. Sun and B. Hu, *Cryst. Growth Des.*, 2023, **24**, 669–677.
43 J. Luo, H. Xia, W. Zhang, S. Song and Q. Zhang, *J. Mater. Chem. A*, 2020, **8**, 12334–12338.
44 D. I. A. Millar, H. E. Maynard-Casely, D. R. Allan, A. S. Cumming, A. R. Lennie, A. J. Mackay, I. D. H. Oswald, C. C. Tang and C. R. Pulham, *CrystEngComm*, 2012, **14**, 3742–3749.
45 J. C. Bennion, N. Chowdhury, J. W. Kampf and A. J. Matzger, *Angew. Chem., Int. Ed.*, 2016, **55**, 13118–13121.
46 C. Yang, L. Chen, S. Chen, W. Wu, W. Yuan, J. Yao, C. Zhang, C. Sun, Y. Du and B. Hu, *Cryst. Growth Des.*, 2021, **21**, 4329–4336.
47 J. Zhou, X. Li, T. Hou, Z. Xu, P. Wang, M. Lu and Y. Xu, *CrystEngComm*, 2023, **25**, 2027–2031.
48 Y. Xu, J. Zhou, X. Li, T. Hou, Z. Xu, P. Wang and M. Lu, *Commun. Mater.*, 2024, **5**, 25.
49 Y. Xu, D. Li, P. Wang, Q. Lin, L. Ding, T. Hou, Y. Yuan and M. Lu, *J. Energ. Mater.*, 2021, **41**, 99–116.
50 Y. Yuan, T. Hou, D. Li, Y. Xu and M. Lu, *Chin. J. Energ. Mater. (Hanneng Cailiao)*, 2022, **30**, 96–102.
51 R. Huang and H. Xu, *Science*, 2018, **359**, eaao3672.
52 C. Jiang, L. Zhang, C. Sun, C. Zhang, C. Yang, J. Chen and B. Hu, *Science*, 2018, **359**, eaas8953.
53 H. Huang, J. Zhong, L. Ma, L. Lv, J. S. Francisco and X. C. Zeng, *J. Am. Chem. Soc.*, 2019, **141**, 2984–2989.
54 W. Chen, Z. Liu, Y. Zhao, X. Yi, Z. Chen and A. Zheng, *J. Phys. Chem. Lett.*, 2018, **9**, 7137–7145.